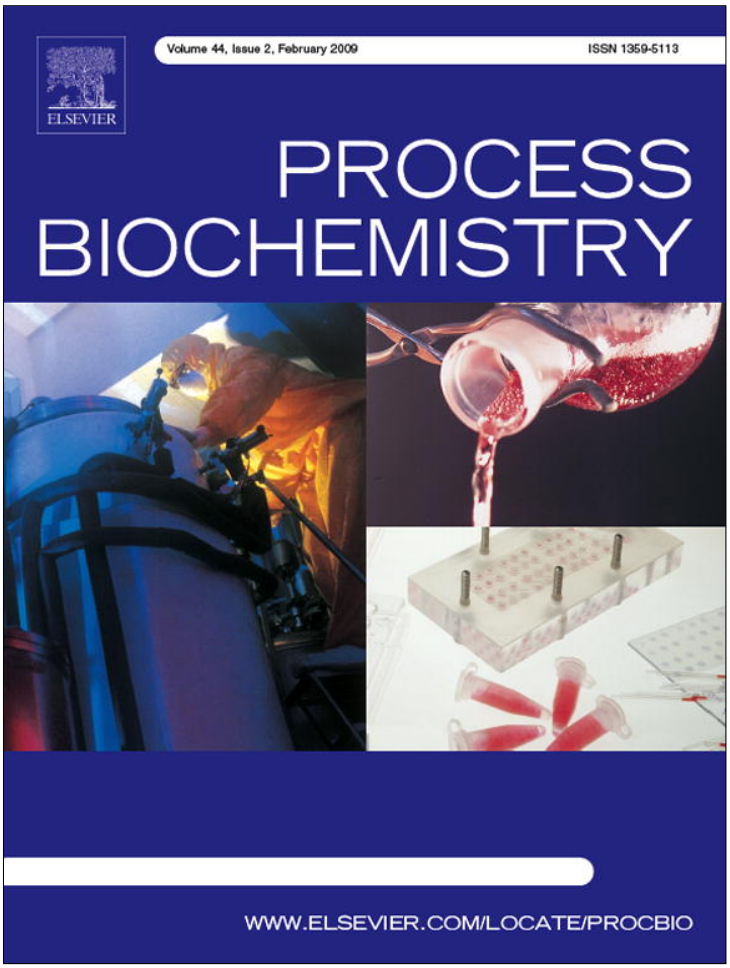

Process Biochemistry 44 (2009) 183–190

Contents lists available at ScienceDirect

Process Biochemistry

journal homepage: www.elsevier.com/locate/procbio

Effect of biocatalyst swelling on the operation of packed-bed immobilized enzyme bioreactor

Enrique J. Mammarella *, Amelia C. Rubiolo

Instituto de Desarrollo Tecnológico para la Industria Química (INTEC), Consejo Nacional de Investigaciones Científicas y Técnicas (CONICET) – Universidad Nacional del Litoral (UNL), Güemes 3450, 3000 Santa Fe. República Argentina

ARTICLE INFO

Article history:
Received 4 June 2008
Received in revised form 8 October 2008
Accepted 9 October 2008

Keywords:
Packed-bed immobilized enzyme reactor
Bed swelling
Mathematical model

ABSTRACT

A general mathematical model was developed for predicting the performance and simulation of a packed-bed immobilized enzyme reactor performing a reaction that follows Michaelis–Menten kinetics with competitive product inhibition. The performance of a packed-bed immobilized enzyme reactor was analyzed taking into account the effect of bed swelling on various diffusional phenomena such as axial dispersion, internal and external mass transfer limitations. The numerical solutions were compared with experimental data obtained for a packed-bed reactor operating with β-galactosidase entrapped in Ca-alginate-K-κ-carrageenan gels for lactose hydrolysis.

1. Introduction

The hydrocolloids are natural carbohydrate polymers of high molecular weight used in the food industry for obtaining important functional properties, such as thickening, hydrogel formation and texture stability. Pectin, gellan, agar-agar, κ-carrageenan and sodium alginate are the most used hydrocolloids among the gelling agents.

Hydrogels are dynamic systems formed by three-dimensional polymer networks. Most hydrogels are produced by ionic or thermal interactions. These materials are very useful in applications such as controlled release of drugs, controlled immobilization, immobilized catalysis, bio-separations, biosensors and artificial tissues. However, hydrogels show phase change or abrupt change in volume due to the environmental changes (temperature, pH, solvent, etc.) [1,2]

The immobilization by entrapment has been accepted as an appropriate technique to fix enzymes when substrate/s and product/s are compounds of low molecular size with high diffusion rates on several supporting hydrocolloid matrices. However, the structure obtained with the hydrocolloids can be modified during the enzymatic reaction by the action of the surrounding medium, producing swelling after weakening the supporting gel.

In some previous works, it was studied the β-galactosidase entrapment process in alginate-carrageenan matrices [3] and the operational stability of this biocatalyst in a packed-bed enzymatic reactor [4]; moreover, the behaviour of some fundamental aspects of the process such as liquid-phase (external) and the solid-phase (internal) mass transfer, intrinsic kinetic parameters, and reactor hydrodynamics in a mathematical model was also analyzed [5]. Because the efficiency of the entrapment can be different due to the modification of the carrier structure, this effect needs to be quantified in the evaluation of the process performance [6].

There are very few papers that analyze the bed swelling on the reactor performance [7–9]. The hydraulic behaviour of a packed-bed and the variation of effective diffusion coefficients in the bed particles were analyzed, but, the effect of competitive inhibition by product on the reaction kinetic was not included in any of the reactor model presented.

The objectives of this work were to study the effect of bed swelling on the performance of a packed-bed immobilized enzyme reactor and validate the simulations with experimental data obtained for lactose hydrolysis using β-galactosidase entrapped in Ca–alginate–K–κ-carrageenan gels.

2. Theory

2.1. Kinetics of enzymatic reaction

A Michaelis–Menten model with competitive inhibition by product (galactose) was used [10].

$$\nu = -\frac{V_{\max}[S]}{\mathrm{Km}(1 + [P]/k_i) + [S]} \quad (1)$$

* Corresponding author. Tel.: +54 342 4511595x1090; fax: +54 342 4511079.
E-mail address: ejoma@intec.unl.edu.ar (E.J. Mammarella).

1359-5113/$ – see front matter © 2008 Elsevier Ltd. All rights reserved.
doi:10.1016/j.procbio.2008.10.009

where $[S]$ is the substrate concentration, V_{max} is the intrinsic maximum reaction rate, Km is intrinsic Michaelis–Menten constant, k_i is the intrinsic inhibition constant by product and $[P]$ is the product concentration, which was considered equal to $[S]_0 - [S]$; $[S]_0$ being the substrate concentration at initial time. It is worth recalling that V_{max} includes information related to $[E]_0$, the concentration of active enzyme at initial time.

2.2. Activity loss of the immobilized enzymes

The activity loss of an immobilized enzyme can occur due to changes in its spatial structure or polypeptide chain ruptures produced by reaction conditions (pH, temperature, ionic force of the reaction medium, etc.), permanent blockade of enzyme active sites by inhibitors or by links to support, steric and solvent effects, enzyme protein loss initially fixed to the support, etc. In this case, a global deactivation that considers all those effects was assumed.

Different mechanisms have been proposed to describe enzyme deactivation [4,11–15]. The simplest and most used is one-stage first-order kinetics, which proposes the transition of a fully active native enzyme to a fully inactivated species in a single step. Such mechanism leads to a model of exponential decay, where the residual enzyme activity at time t can be determined by

$$[E] = [E]_0 \, e^{-k_d t} \tag{2}$$

where $[E]_0$ and $[E]$ are the concentrations of active enzyme at initial time and at any other time, respectively, and k_d is the deactivation rate constant, which follows the Arrhenius equation for the temperature dependence.

2.3. Mass balance in the reactor

The mathematical model that describes the behaviour of the packed-bed immobilized enzyme reactor was formulated using the following assumptions:

(a) an isothermal packed-bed immobilized enzyme reactor, operating in steady state,
(b) the spherical particles are uniformly packed in the reactor,
(c) the hydrodynamics of the fluid in the reactor is described by dispersed plug-flow model,

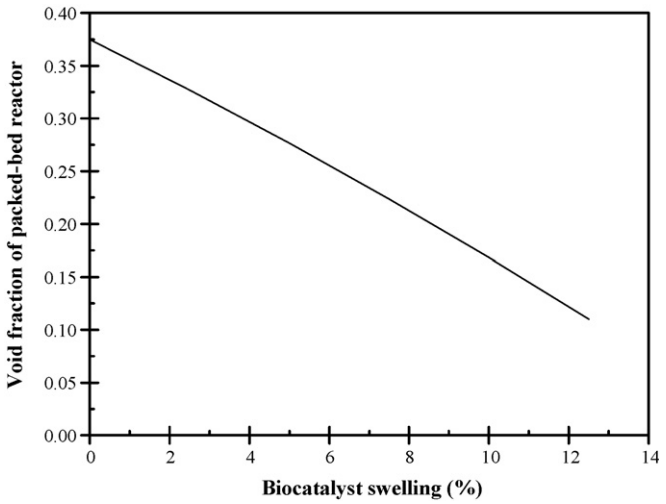

Fig. 1. Effect of biocatalyst swelling on the void fraction of packed-bed reactor.

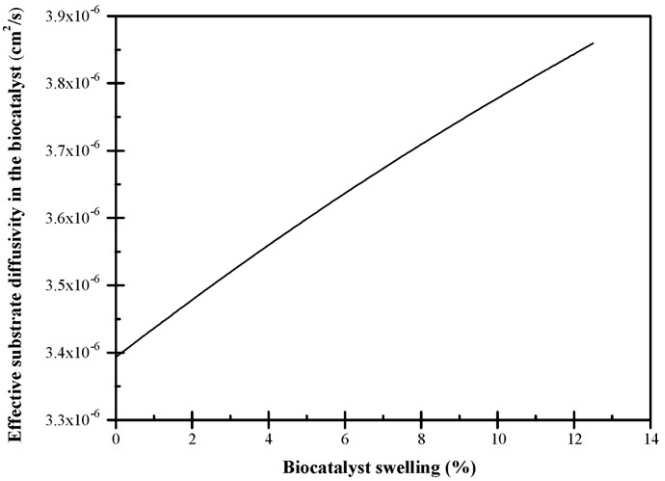

Fig. 2. Effect of biocatalyst swelling on effective substrate diffusivity in the biocatalyst.

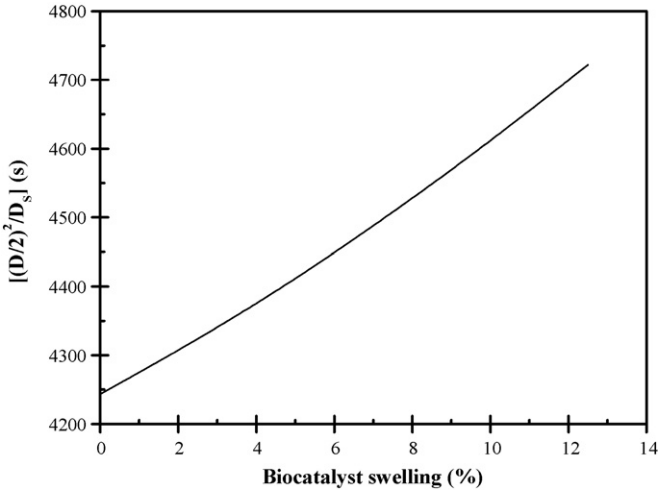

Fig. 3. Effect of biocatalyst swelling on structural resistance to diffusion represented by the relationship between the square of particle radius and the effective substrate diffusivity in the biocatalyst.

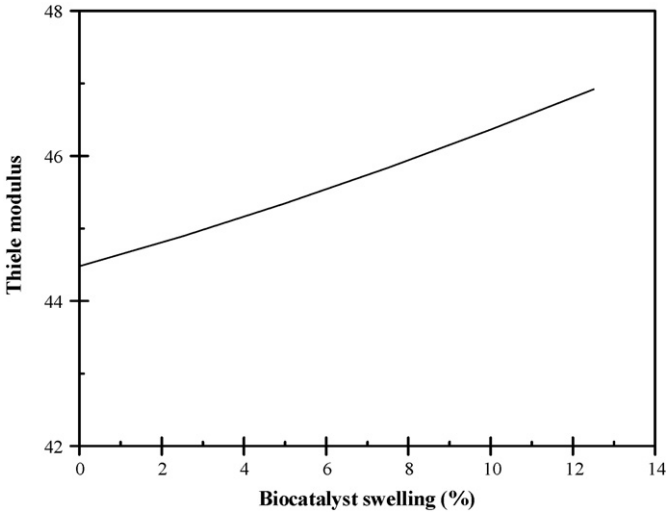

Fig. 4. Effect of biocatalyst swelling on Thiele modulus.

(d) the pressure drop across the reactor and the radial concentration gradient in the bulk fluid phase are negligible,
(e) the superficial velocity is uniform with position in the reactor,
(f) the lactose hydrolysis is an enzymatic reaction that uses one substrate and yields only two products,
(g) the kinetics of lactose hydrolysis is described by a Michaelis–Menten model with competitive inhibition by product, as shown in Eq. (1),
(h) one-stage first-order kinetics for enzyme deactivation,
(i) the enzyme activity is uniform throughout the particle and the reactor,

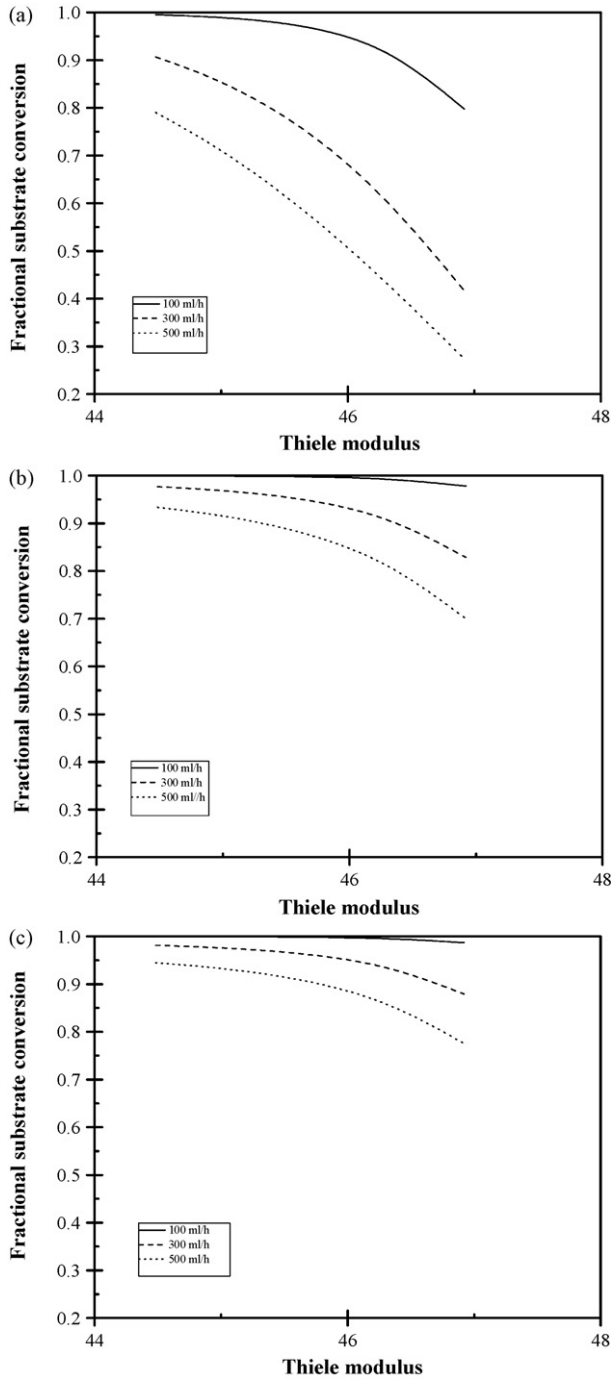

Fig. 5. Effects of Thiele modulus on reactor conversion for different feed flow rate and different $[S]_0^b/Km$ (a: $[S]_0^b/Km = 10$, b: $[S]_0^b/Km = 1$ and c: $[S]_0^b/Km = 0.1$).

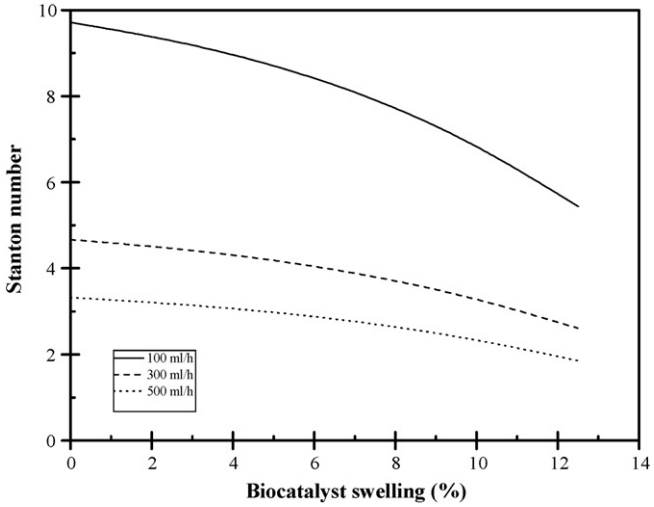

Fig. 6. Effect of biocatalyst swelling on Stanton number for different feed flow rate.

(j) partitioning coefficients at surface particle are equal to unity,
(k) the substrate and product diffusion inside the catalytic particle follows Fick's law,
(l) the effective substrate and product diffusivities in the catalytic particles are equal,
(m) the effective diffusivity does not change throughout the particles and it is independent of the concentration.

Therefore, the mass balance equation for obtaining the substrate concentration profile in the liquid stream (b) in an isothermal packed-bed reactor of a length Z, can be written:

$$D_z \frac{\partial^2 [S]^b}{\partial z^2} - u_z \frac{\partial [S]^b}{\partial z} = v \tag{3}$$

with boundary conditions:

$$z = 0^+ \quad [S]^b - [S]_0^b = \frac{D_z}{u_z} \frac{\mathrm{d}[S]^b}{\mathrm{d}z} \tag{4}$$

$$z = Z \quad \frac{\mathrm{d}[S]^b}{\mathrm{d}z} = 0 \tag{5}$$

where D_z is the axial dispersion coefficient, z is the axial coordinate, u_z is the superficial fluid velocity in the reactor, and $[S]_0^b$ is the substrate concentration at initial time in the liquid stream.

Considering the enzyme deactivation, Eq. (1) becomes

$$v = \frac{-V_{max}[S]}{Km(1 + [P]/k_i) + [S]} = \frac{-[E]_0^i \, e^{-k_d t} k_2 [S]}{Km\left(1 + ([S]_0^b - [S]^b)/k_i\right) + [S]} \tag{6}$$

Taking into account that there is not a conformational change in the enzyme during the entrapment method used for the immobilization, Km and k_i are the values corresponding to the free enzyme, that is, the main effect on the reaction rate is the mass transfer [5].

Using Eq. (6) and dimensionless variables, $C^* = [S]^b/[S]_0^b$, $C = [S]/[S]_0^b$, Pe = $u_z Z/D_z$, and $x = z/Z$, Eq. (3) becomes

$$\frac{[S]_0^b}{Pe} \frac{\mathrm{d}^2 C^*}{\mathrm{d}x^2} - \frac{\mathrm{d}C^*}{\mathrm{d}x} - \frac{Z}{u_z} \frac{[E]_0^i \, e^{-k_d t} k_2 C}{Km\left[1 + [S]_0^b (1 - C)/k_i\right] + [S]_0^b C} = 0 \tag{7}$$

To solve this equation, the dimensionless substrate concentration inside the biocatalyst spherical particle, C, should be known; therefore, a mass balance considering diffusion and chemical

reaction in steady state in the particles was considered:

$$\frac{1}{r^2}\frac{d}{dr}\left(r^2 D_S \frac{d[S]}{dr}\right) = -\nu \tag{8}$$

where D_S is the effective diffusion coefficient of the substrate in the biocatalyst particle. The boundary conditions are

$$r = 0 \quad \frac{d[S]}{dr} = 0 \tag{9}$$

$$r = R \quad \frac{d[S]}{dr} = \frac{k_l}{D_S}([S]^b - [S]) \tag{10}$$

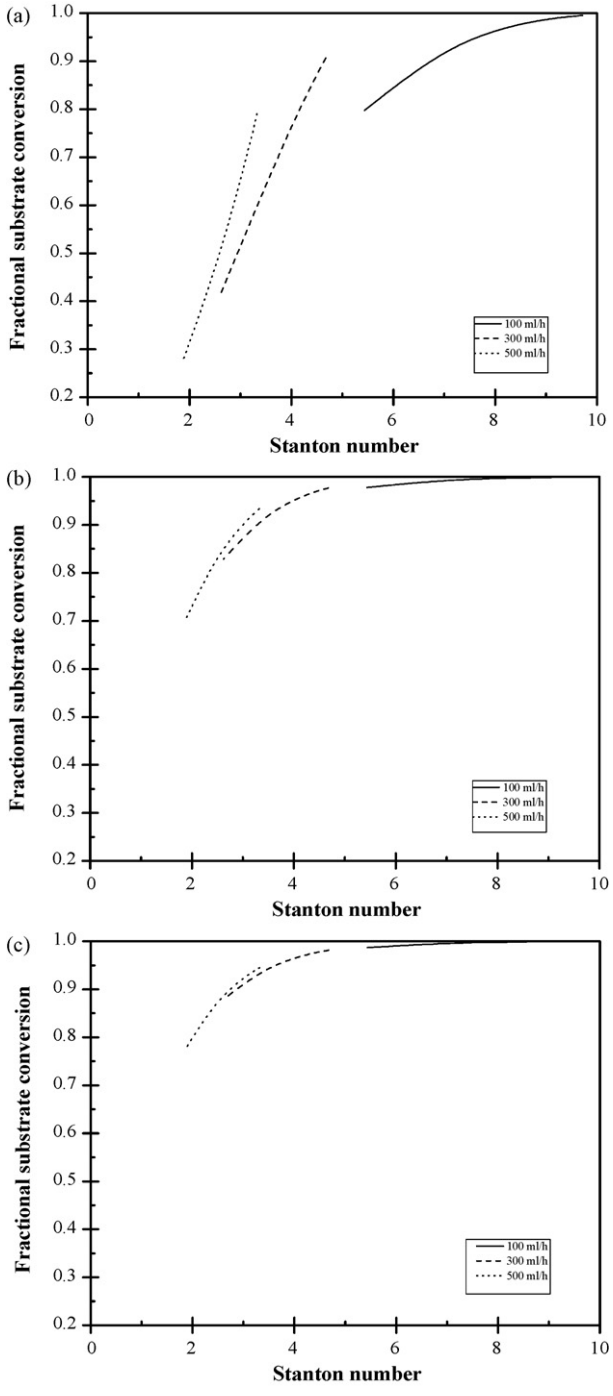

Fig. 7. Effects of Stanton number on reactor conversion for different feed flow rate and different $[S]_0^b/Km$ (a: $[S]_0^b/Km = 10$, b: $[S]_0^b/Km = 1$ and c: $[S]_0^b/Km = 0.1$).

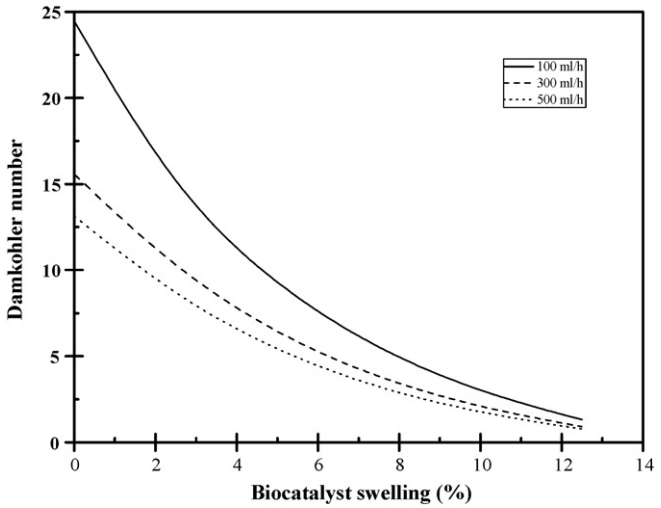

Fig. 8. Effect of biocatalyst swelling on Damkohler number for different feed flow rate.

where k_l is the external mass transfer coefficient. Using the dimensionless variables:

$$y = \frac{r}{R}, \quad \Phi^2 = \frac{V_{max}R^2}{Km\,D_S}, \quad \gamma = \frac{[S]_0^b}{Km}, \quad \gamma_2 = \frac{[S]_0^b - [S]}{k_i}$$
$$\gamma_2' = \frac{[S]_0^b}{k_i}, \quad \varphi = \frac{u_z R^2}{D_S Z}, \quad \varphi_2 = \frac{u_z R^2 [S]_0^b}{Pe\,D_S Z}, \quad Bi = \frac{k_l R}{D_S} \tag{11}$$

Eq. (7) results

$$\varphi_2 \frac{d^2C^*}{dx^2} - \varphi \frac{dC^*}{dx} = \frac{\Phi^2 C}{1 + \gamma C + \gamma_2'(1 - C)} \tag{12}$$

with the following boundary conditions:

$$x = 0 \quad C^* = 1 + \frac{\varphi_2}{\varphi [S]_0^b}\frac{dC^*}{dx} \tag{13}$$

$$x = 1 \quad \frac{dC^*}{dx} = 0 \tag{14}$$

Therefore, Eq. (8) results

$$\frac{d^2C}{dy^2} = \frac{\Phi^2 C}{1 + \gamma_2 + \gamma C} \tag{15}$$

with the following boundary conditions:

$$y = 0 \quad \frac{dC}{dy} = 0 \tag{16}$$

$$y = 1 \quad C = 1 - \frac{1}{Bi}\frac{dC}{dy} \tag{17}$$

The method of orthogonal collocation with six internal points for the reactor axial direction and six internal points for the biocatalyst particle were used to solve the system (12)–(17) [16]. The number of collocation points was chosen to ensure a satisfactory convergence.

2.4. Criteria for reactor performance

To evaluate the reactor performance, the following variables were calculated:

Conversion is defined as the ratio between the total moles of substrate converted into product and the total moles of substrate

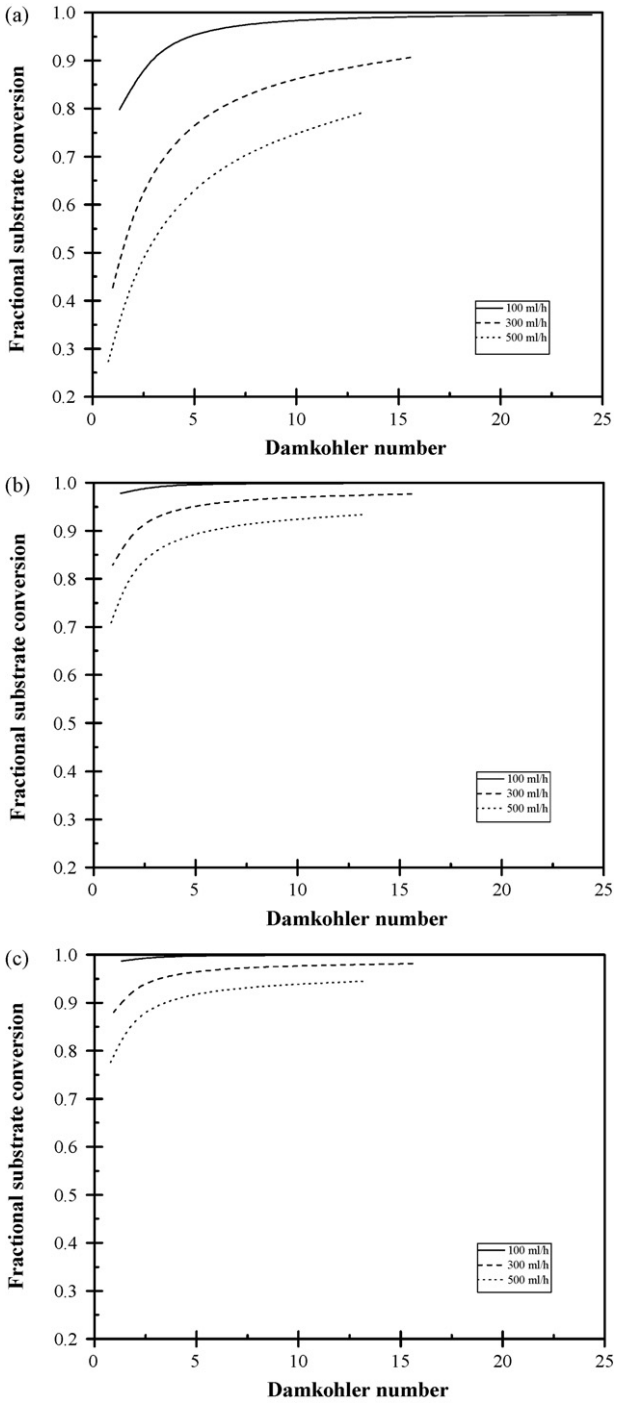

Fig. 9. Effects of Damkohler number on reactor conversion for different feed flow rate and different $[S]_0^b$/Km (a: $[S]_0^b$/Km = 10, b: $[S]_0^b$/Km = 1 and c: $[S]_0^b$/Km = 0.1).

fed into the reactor as follows:

$$X = 1 - \left([S]^b/[S]_0^b\right) \tag{18}$$

Yield is defined as the ratio of the substrate converted to the maximum amount that could be converted during one residence time as follows:

$$Y = \frac{[S]_0^b - [S]_Z^b}{V_{\max}(\varepsilon Z/u_z)} \tag{19}$$

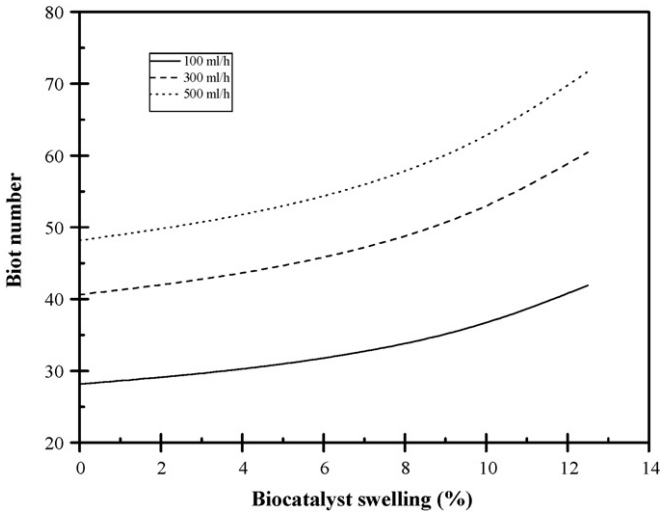

Fig. 10. Effect of biocatalyst swelling on Biot number for different feed flow rate.

where $[S]_Z^b$ is the substrate concentration at reactor outlet and ε is the void fraction of the packed-bed reactor.

3. Results and discussion

For the analysis of swelling effect on reactor performance, substrate conversion and yield are calculated as a function of dimensionless parameters: Thiele modulus (ϕ), Stanton number (St), Damkohler number (Da), Peclet number (Pe), and mass transfer Biot number (Bi) [17].

The ϕ represents internal mass transfer limitations, St and Da represent external mass transfer limitations, and Bi represents simultaneous interaction between internal and external mass transfer.

The experimental results were obtained and analyzed using the reactor design, work conditions and kinetic constants already described [3–5]. The parameters of this system were:

(a) reactor parameters: Z = 34.0 cm, useful volume = 57.80 cm^3,
(b) kinetics parameters: Km = 0.190 M, k_i = 0.099 M, $k_2 = 5 \times 10^{-4}$ mol l^{-1} min^{-1} mg^{-1} protein, k_d = 0.0180 h^{-1},
(c) bed parameters: biocatalyst mass = 38.94 g, initial total biocatalyst volume = 36.06 cm^3, initial biocatalyst diameter = 0.240 cm, initial retention of enzyme protein per gram of biocatalyst = 4.55×10^{-3} g, biocatalyst swelling = 0.0%, 2.5%, 5.0%, 7.5%, 10.0% and 12.5%,
(d) substrate parameters: $[S]_0^b$ = 1.900, 0.190 and 0.019 M; diffusion coefficient at infinite dilution in water at 25 °C = 5.21×10^{-6} cm^2 s^{-1}, feed flow rate = 100, 300 and 500 ml h^{-1}.

The correlation proposed by Chilton and Colburn was used for the prediction of mass transfer coefficient of lactose [18]. The axial dispersion coefficient was estimated with the method used by Levenspiel [19]. The effective diffusion coefficient of substrate into biocatalyst was calculated according to Axelsson et al. [20].

The reactor hydrodynamics is characterized by Pe, which represents the axial dispersion effects. The Pe is the ratio of backmixing time to residence time. It measures the effect of degree of mixing, for extremely low Pe (i.e. Pe = 0.001) it represents CSTR, for high Pe (i.e. Pe = 10^4) it represents PFR and dispersed plug-flow reactor model (DPFR) characterized by finite Pe. In this case, the Pe value was maintained in the value of 32.3.

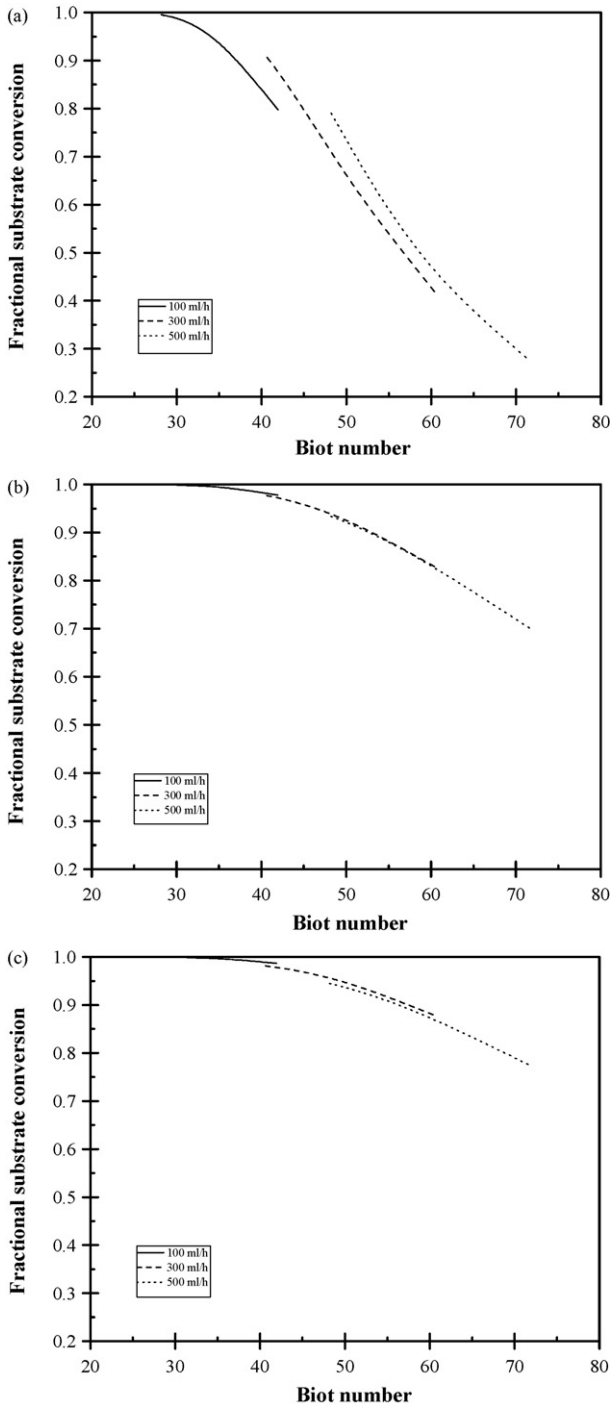

Fig. 11. Effects of Biot number on reactor conversion for different feed flow rate and different $[S]_0^b$/Km (a: $[S]_0^b$/Km = 10, b: $[S]_0^b$/Km = 1 and c: $[S]_0^b$/Km = 0.1).

Fig. 1 shows a non-linear effect of biocatalyst swelling on the void fraction of packed-bed reactor. As it can be observed, an increase in the biocatalyst swelling reduces significantly the void fraction in the reactor, and the effect on the residence time of substrate in the reactor could be important when the initial feed flow rate is increased. The initial void fraction of packed bed reactor, obtained by the relationship between the initial total biocatalyst volume and the useful volume of the reactor, was 0.3750.

Fig. 2 shows the effect of biocatalyst swelling on the effective substrate diffusivity in the biocatalyst. As it is expected, the predicted value for the effective substrate diffusion coefficient in the gel particle is smaller than the value obtained for infinitely dilute solution, mainly due to the steric hindrance of the random movement of the substrate in the gel matrix. Moreover, according to Axelsson et al. [20], due to the biocatalyst swelling process, the effective solid fraction in the gel matrix is progressively reduced; the value of the effective substrate diffusion coefficient in the gel particle being higher and progressively increased in a non-linear form.

The effect of biocatalyst swelling on structural resistance to diffusion represented by the relationship between the square of particle radius and the effective substrate diffusivity in the biocatalyst is shown in Fig. 3. As it is observed, the swelling process produces a non-linear increasing in the structural resistance that can be assumed as a residence time of the substrate into the gel particle and that affects negatively the reaction rate.

The Thiele modulus describes a ratio between kinetic rate and diffusional rate. For this paper, a generalizated relation for the Thiele modulus can be presented as a linear function of the particle radium and proportional to the inverse square root of the effective diffusion coefficient of the substrate in the biocatalyst particle. Fig. 4 shows the effect of biocatalyst swelling on Thiele modulus. As the biocatalyst swelling increases, a non-linear increasing of ϕ is obtained due to the increased in the effective diffusion coefficient of the substrate in the biocatalyst particle. Moreover, for the conditions studied, the internal effectiveness factor, obtained graphically using the methodology proposed by Pitcher [21], was between 0.02 and 0.05.

Fig. 5 shows the effect of Thiele modulus on the fractional substrate conversion in the reactor. As it is observed, when the ϕ value increases, the fractional substrate conversion in the reactor decreases for the feed flow rate studied. In fact, it is difficult to predict this effect due to the swelling process, the Thiele modulus is affected in a different way by changes in the particle radius, of the effective substrate diffusion coefficient and the effective enzyme concentration into the gel particle.

The effect of biocatalyst swelling on St is shown in Fig. 6. The biocatalyst swelling produces a reduction in St. The St is a relation between the external mass transfer resistance and the residence time. For the analyzed conditions, the residence time decreases more that external mass transfer resistance and that ratio is not linear.

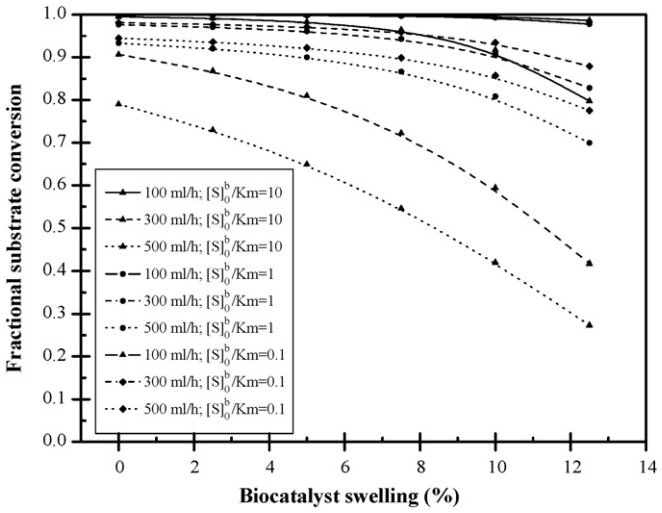

Fig. 12. Effect of biocatalyst swelling on reactor conversion for different feed flow rate and different $[S]_0^b$/Km.

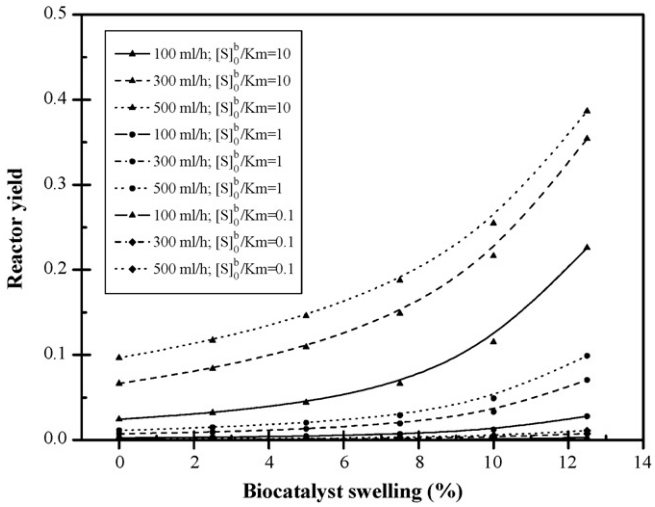

Fig. 13. Effect of biocatalyst swelling on reactor yield for different feed flow rate and different $[S]_0^b$/Km.

The dependence of substrate conversion with St was studied (Fig. 7). The substrate conversion increases when increasing St. Moreover, for high values of ϕ and St, when the mass transfer limitations are controlling the process, the substrate conversion is independent of substrate concentration. Higher substrate conversion is achieved when increasing St because external mass transfer is increased, that is, the external mass transfer resistance is reduced.

Fig. 8 shows the effects of biocatalyst swelling on Da. As the biocatalyst swelling increases, a non-linear decreasing in Da is obtained.

Due to biocatalyst swelling process increases the particle diameter, the superficial fluid velocity is increased and external mass transfer resistance is reduced affecting the substrate conversion in the reactor. For Da values higher than 10, substrate conversions higher than 0.90 are obtained (Fig. 9).

The effect of biocatalyst swelling on Bi is shown in Fig. 10. The biocatalyst swelling produces a non-linear increasing in Bi. Higher substrate conversions are achieved for Bi values lower than 40. At high Bi values, the radial substrate profiles in the particles are most pronounced, affecting the reactor conversion (Fig. 11). As Bi increases, the external mass transfer resistance decreases.

The global effect of biocatalyst swelling on reactor conversion is shown in Fig. 12. The biocatalyst swelling produces a non-linear decreasing in reactor conversion. For each feed flow rate, a biocatalyst swelling value from which the reactor conversion decreases quickly can be observed.

Fig. 13 displays the global yield with respect to biocatalyst swelling for different feed flow rates. The global yield increases when increasing biocatalyst swelling. It can be observed that the maximum yield is obtained for higher biocatalyst swelling at 500 ml h^{-1} of feed flow rate. However, that might be a point of low productivity due to low reactor conversion.

Theoretical predictions were determined for the same variables used to obtain experimental data. Theoretical prediction and experimental data for substrate conversion obtained in the same conditions are shown in Table 1. As it is observed, for the conditions studied, the theoretical model predicted the experimental behaviour with smaller error.

Table 1
Simulated and experimental lactose conversion values.

$[S]_0^b$ (M)	Biocatalyst swelling (%)	Feed flow rate (ml h^{-1})	Fractional substrate conversion	
			Experimental	Predicted
1.90	0.00	100	1.000	0.995
		300	0.920	0.907
		500	0.790	0.790
	5.00	100	0.990	0.983
		300	0.825	0.810
		500	0.645	0.649
	10.00	100	0.930	0.918
		300	0.590	0.594
		500	0.425	0.419
0.19	0.00	100	1.000	0.999
		300	0.990	0.977
		500	0.945	0.934
	5.00	100	1.000	0.999
		300	0.970	0.961
		500	0.915	0.900
	10.00	100	1.000	0.993
		300	0.915	0.907
		500	0.790	0.800

4. Conclusions

Catalytic particle size plays a key role in the design of immobilized enzyme processes. The effect of bed swelling, mass transfer limitations and axial dispersion was considered in a mathematical model for a packed-bed immobilized enzyme reactor.

The effect of Thiele modulus (ϕ), Stanton number (St), Damkohler number (Da), Peclet number (Pe) and Biot number (Bi) were studied. The reactor conversion is almost complete for high Da and St. Furthermore; it is found that substrate conversion decreases when increasing biocatalyst swelling.

The maximum yield is obtained for higher biocatalyst swelling at 500 ml h^{-1} of feed flow rate. However, that might be a point of low productivity due to low reactor conversion.

The information obtained by simulations is a valuable tool for immobilized enzyme reactor design by providing a quantitative relation of enzyme performance changing operational variables. The model predicted the experimental data with errors smaller than 2.5%.

Acknowledgments

This work was done with the financial support of Universidad Nacional del Litoral (Santa Fe, Argentina), Consejo Nacional de Investigaciones Científicas y Técnicas (Argentina) and Agencia Nacional de Promoción Científica y Tecnológica (Argentina).

Appendix A. Nomenclature

Species

E enzyme
P product
S substrate

Variables

γ dimensionless variable, $[S]_0^b$/Km
γ_2 dimensionless variable, $([S]_0^b - [S])/k_i$
γ'_2 dimensionless variable, $[S]_0^b/k_i$
ε void fraction of packed bed reactor

ν reaction rate term
φ dimensionless variable, $u_z R^2/(D_s Z)$
φ_2 dimensionless variable, $u_z R^2 [S]_0^b/(\mathrm{Pe} D_S Z)$
Φ Thiele modulus, $R\sqrt{V_{\max}/(\mathrm{Km}\, D_S)}$
Φ^2 dimensionless variable, $V_{\max} R^2/(\mathrm{Km}\, D_S)$
a specific area of the spherical biocatalyst particle (cm^{-1})
Bi mass transfer Biot number, $k_l R/D_s$
C dimensionless substrate concentration inside biocatalyst particle, $[S]/[S]_0^b$
C^* dimensionless substrate concentration in the liquid stream, $[S]^b/[S]_0^b$
D biocatalyst particle diameter (cm)
Da Damkohler number, $\frac{\varepsilon}{(1-\varepsilon)} \frac{V_{\max}}{Km\, k_l a}$
D_S effective substrate diffusion coefficient ($\mathrm{cm}^2\ \mathrm{s}^{-1}$)
D_z axial dispersion coefficient ($\mathrm{cm}^2\ \mathrm{s}^{-1}$)
k_2 intrinsic constant for Michelis–Menten kinetic equation ($\mathrm{mol\ l}^{-1}\ \mathrm{min}^{-1}\ \mathrm{mg}^{-1}$ protein)
k_d deactivation rate constant (h^{-1})
k_i intrinsic inhibition constant by product ($\mathrm{mol\ l}^{-1}$)
k_l external mass transfer coefficient ($\mathrm{cm\ s}^{-1}$)
Km intrinsic Michaelis–Menten constant ($\mathrm{mol\ l}^{-1}$)
Pe Peclet number, $u_z Z/D_z$
r radial coordinate (cm)
R biocatalyst particle radium (cm)
St Stanton number, $(1-\varepsilon) k_l\, aZ/u_z$
t operation time (h)
u_z superficial fluid velocity in the reactor ($\mathrm{cm\ s}^{-1}$)
$V_{\max}$ intrinsic maximum reaction rate ($\mathrm{mol\ l}^{-1}\ \mathrm{min}^{-1}$)
x dimensionless axial coordinate, z/Z
X substrate conversion
y dimensionless radial coordinate, r/R
Y reactor yield
z axial coordinate (cm)
Z reactor length (cm)

Symbols

[] Concentration ($\mathrm{mol\ l}^{-1}$)

Subindexes

0 at initial time
aq in water

Subscripts

b in the liquid stream
i immobilized

References

[1] Luh N, Flink J, Karel M. Fabrication, characterization, and modification of the texture of calcium alginate gels. J Food Sci 1977;42:976–81.
[2] Woodward J, Krasniak S, Smith R, Spielberg F, Zachry G. Preparation and characterization of β-D-glucosidase immobilized in calcium alginate. Biotechnol Bioeng Symp 1982;12:485–9.
[3] Mammarella E, Rubiolo A. Response surface methodology to optimize β-galactosidase immobilization using a combination of hydrocolloids as the supporting matrix. Biotechnol Prog 1996;12:612–7.
[4] Mammarella E, Rubiolo A. Study of the deactivation of β-galactosidase entrapped in alginate-carrageenan gels. J Mol Catal B Enzym 2005;34:7–13.
[5] Mammarella E, Rubiolo A. Predicting the packed-bed reactor performance with immobilized microbial lactase. Process Biochem 2006;41:1627–36.
[6] Doherty E, Halling P, McNeil B. Physiology of immobilised cells. Amsterdam, Netherlands: Elsevier; 1990.
[7] Tuncel A. An engineering analysis for the continuous reactor behaviour of α-chymotrypsin-immobilized thermosensitive gel cylinders. J Biotechnol 1998; 63:41–54.
[8] Shadday M. A one-dimensional transient model of down-flow through a swelling packed porous bed. Chem Eng Sci 2006;61:2688–700.
[9] Sainio T, Paatero E. Mass coordinates for dynamic simulation of column operation involving dimensional changes of packing material. Comp Chem Eng 2007;31:374–83.
[10] Carrara C, Mammarella E, Rubiolo A. Prediction of the fixed-bed reactor behaviour using dispersion and plug-flow models with different kinetics for immobilised enzyme. Chem Eng J 2003;92:123–9.
[11] Henley S, Sadana T. Deactivation theory. Biotechnol Bioeng 1986;28:1277–85.
[12] Illanes A, Wilson L, Altamirano C, Aillapán A. Reactor performance under thermal inactivation and temperature optimization with chitin-immobilized lactase. In: Progress in biotechnology, vol. 15. Stability and stabilization of biocatalysts. Amsterdam, Netherlands: Elsevier; 1998.
[13] Giacomini C, Irazoqui G, Batista-Viera F, Brena B. Influence of the immobilization chemistry on the properties of immobilized β-galactosidases. J Mol Catal B Enzym 2001;11:597–606.
[14] Brena B, Irazoqui G, Giacomini C, Batista-Viera F. Effect of increasing co-solvent concentration on the stability of soluble and immobilized β-galactosidase. J Mol Catal B Enzym 2003;21:25–9.
[15] Rodriguez-Nogales J, Delgadillo A. Stability and catalytic kinetics of micro-encapsulated β-galactosidase in liposomes prepared by the dehydration–rehydration method. J Mol Catal B Enzym 2005;33:15–21.
[16] Finlayson BA. Nonlinear analysis in chemical engineering. New York, USA: McGraw-Hill; 1980.
[17] Al-Muftah AE, Abu-Reesh IM. Effects of simultaneous internal and external mass transfer and product inhibition on immobilized enzyme-catalyzed reactor. Biochem Eng J 2005;27:167–78.
[18] Geankoplis C. Procesos de transporte y operaciones unitarias. México, México: Compañía Editorial Continental S.A. de C.V; 1999.
[19] Levenspiel O. The chemical reactor omnibook. Corvallis, USA: OSU Book Stores; 1979.
[20] Axelsson A, Sisak C, Westrin B, Szajáni B. Diffusional characteristics of a swelling gel and its consequences for bioreactor performance. Chem Eng J 1994;55:B35–9.
[21] Pitcher W. Design and analysis of immobilized enzyme reactor. In: Immobilized enzymes for industrial reactors. Oxford, UK: Academic Press; 1975.